Supplementary Information

High-property anode catalyst compositing Co-based perovskite and NiFe-layered double hydroxides for alkaline seawater splitting

Ruigan Hu ‡ [a], Fuyue Liu ‡ [a], Haoqi Qiu [a], He Miao [a,] *, Qin Wang [b], Houcheng Zhang [b], Fu Wang [a], Jinliang Yuan [a]

[a] Faculty of Maritime and Transportation, Ningbo University, Ningbo 315211, PR China

[b] Department of Microelectronic Science and Engineering, Faculty of Science, Ningbo University, Ningbo 315211, PR China

*Corresponding author:

Prof. He Miao, E-mail: miaohe@nbu.edu.cn

‡ These authors contributed equally to this work

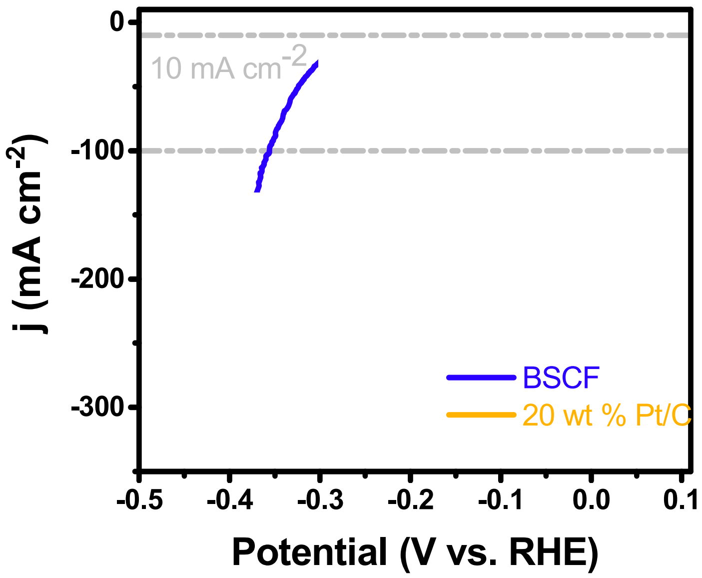

Figure S1. HER performances comparison of BSCF and 20 wt% Pt/C.

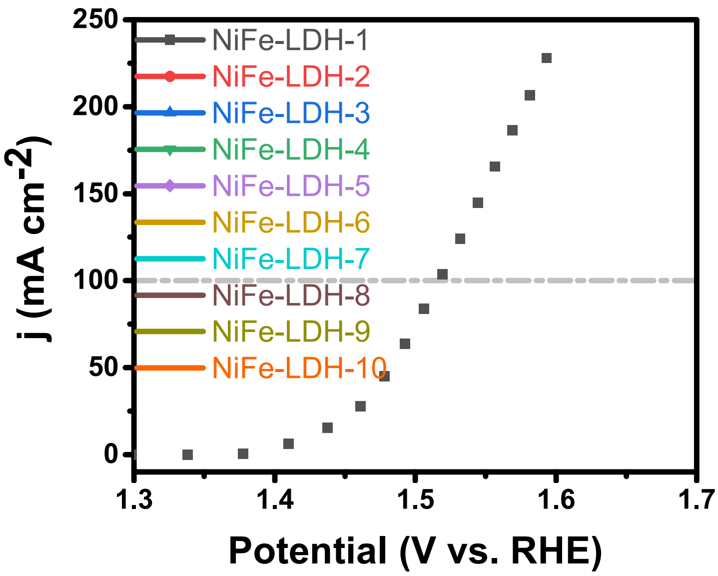

Figure S2. 10 Consecutive LSV curves of catalyst NiFe-LDH at the different measuring times.

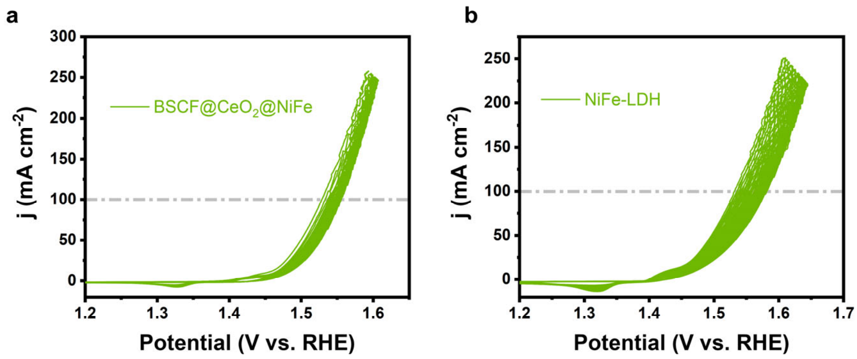

Figure S3. CV curves of (a) BSCF@CeO_2@NiFe-113 and (b) NiFe-LDH at continuous 25-cycle tests.

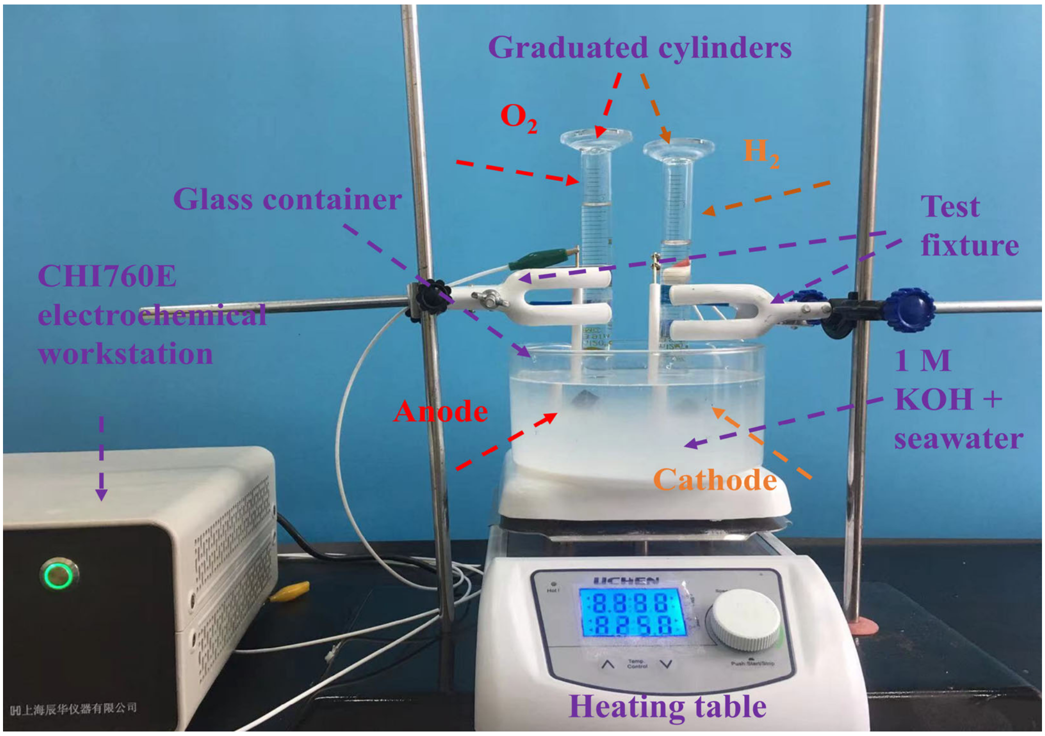

Figure S4. Diagram of oxygen evolution Faraday Efficiency test device.

Specifically, the gas volume (V_{mea}, mL) of oxygen evolution and hydrogen evolution per 20 min is measured with a graduated cylinder. Then, the corresponding calculation is performed according to the Faraday efficiency (FE) formula:

$$\text{Faraday Efficiency} = \frac{m \times n \times F}{I \times t}. \tag{S1}$$

Where the *m* is the actual number of moles of the product, *n* is the number of reaction electrons (n = 4 for OER, n = 2 for HER), *F* is the Faraday constant (*F*=96485.3383 ± 0.0083 C mol^{-1}), *I* is current, *t* is time and the subscript notation $_{mea}$ is 'measured'. The theoretical oxygen evolution and hydrogen evolution Faradaic efficiency is 100 %. The mole and actual FE conversions of the generated gas is based on:

$$\mathrm{m_{mea}} = \frac{\mathrm{V_{mea}}}{\mathrm{V_{m'}}} \text{(mmol)}, \tag{S2}$$

$$\mathrm{V_{m'}} = 22.4655\ \mathrm{L\ mol^{-1}}\ \text{(under normal temperature and pressure)}, \tag{S3}$$

$$\mathrm{FE} = \frac{\mathrm{m_{mea}}}{m} \times 100\ \%. \tag{S4}$$

Table S1. The main compositions in natural seawater[1].

Species	Conc. [mol kg_{H2O}^{-1}]	Conc. [g kg_{H2O}^{-1}]
H_2O	/	/
Na^+	0.48616	11.1768
Cl^-	0.56576	20.0579

Table S2. OER performance comparison of BSCF with other perovskites.

Catalysts	$E_{j=10}$ (V)	Tafel slope (mV dec^{-1})	$E_{j=100}$ (V)	Electrolyte	Substrate	Reference
BSCF	1.56	61.4	1.65	1 M KOH	Glassy carbon	This work
SNCF-NRs	1.60	48	~1.67	1 M KOH	Glassy carbon	[2]
NBCCFe	~1.57	N. A. *	1.68	1 M KOH	Carbon paper	[3]
3C-$SrIrO_3$	1.54	74	N. A.	1 M KOH	Glassy carbon	[4]
Sr_2FeIrO_6	1.60	80	N. A.	1 M KOH	Glassy carbon	[4]
$CaCoO_3$	~1.56	N. A.	~1.63	1 M KOH	Glassy carbon	[5]
$SrCoO_3$	~1.57	N. A.	~1.65	1 M KOH	Glassy carbon	[5]
$LaCoO_3$	1.78	N. A.	N. A.	1 M KOH	Glassy carbon	[5]
$PrBaCo_{0.8}W_{0.2}$	1.55	79.33	N. A.	1 M KOH	Glassy carbon	[6]
PrBaCo	1.62	63.88	N. A.	1 M KOH	Glassy carbon	[6]
BSCF	1.56	119.73	N. A.	1 M KOH	Glassy carbon	[7]
IrO_2	1.58	81	~1.74	1 M KOH	Glassy carbon	[8]

*: N. A.= Not available.

Table S3. Comparison of the OER activities of the different types of perovskite composites in this work and the other reports.

Catalysts	$E_{j=10}$ (V)	Tafel slope (mV dec^{-1})	$E_{j=100}$ (V)	Electrolyte	Preparation method	Reference
BSCF	1.56	61.4	1.65	1 M KOH	Sol-gel	This work
BSCF@CeO_2	1.52	47.3	1.64	1 M KOH	Composite	This work
BSCF@CeO_2@NiFe	1.46	47.1	1.52	1 M KOH	Composite	This work
BSCF@NiFe(-LDH)	1.47	58.5	1.57	1 M KOH	Composite	This work
NiFe-LDH	1.46	71.9	1.54	1 M KOH	Coprecipitation	This work
SNCF-NRs	1.60	48	~1.67	1 M KOH	Electrospinning	[2]
$Ni_{0.66}Fe_{0.33}$ LDH	1.478	46	1.65	1 M KOH	Coprecipitation	[9]
BSCF/NiFe-25	1.56	52.9	~1.64	1 M KOH	Composite	[10]
BSCF-80-ES	1.54	N. A. *	N. A.	1 M KOH	Electrospinning	[11]
PBMNC/LDH-20	1.60	108.6	~1.745	1 M KOH	Composite	[12]
BSCF-Ag	1.67	122	N. A.	1 M KOH	Doping	[13]
F-BSCF	1.51	102.65	~1.68	1 M KOH	Doping	[7]
p-$Cu_{1-x}NNi_{3-y}$/FeNiCu	1.51	52	~1.64	1 M KOH	Doping	[14]
CQD/NiFe-LDH	1.465	35	N. A.	1 M KOH	Composite	[15]
CQDs@BSCF-NFs	1.58	66	~1.645	1 M KOH	Composite	[16]
L-0.5/rGO	1.568	80	~1.68	1 M KOH	Composite	[17]
a-LNF(t-d)	1.48	36	~1.545	1 M KOH	A top-down strategy	[18]

*: N. A.= Not available.

Reference

1. Dresp, S.; Dionigi, F.; Klingenhof, M.; Strasser, P. Direct Electrolytic Splitting of Seawater: Opportunities and Challenges. *ACS Energy Letters* **2019**, *4*, 933-942, doi:10.1021/acsenergylett.9b00220.
2. Zhu, Y.; Zhou, W.; Zhong, Y.; Bu, Y.; Chen, X.; Zhong, Q.; Liu, M.; Shao, Z. A Perovskite Nanorod as Bifunctional Electrocatalyst for Overall Water Splitting. *Advanced Energy Materials* **2017**, *7*, doi:10.1002/aenm.201602122.
3. Kim, N.-I.; Cho, S.-H.; Park, S.H.; Lee, Y.J.; Afzal, R.A.; Yoo, J.; Seo, Y.-S.; Lee, Y.J.; Park, J.-Y. B-site doping effects of NdBa0.75Ca0.25Co2O5+δ double perovskite catalysts for oxygen evolution and reduction reactions. *Journal of Materials Chemistry A* **2018**, *6*, 17807-17818, doi:10.1039/c8ta06236f.
4. Ye, X.; Song, S.; Li, L.; Chang, Y.-C.; Qin, S.; Liu, Z.; Huang, Y.-C.; Zhou, J.; Zhang, L.-j.; Dong, C.-L.; et al. A′–B Intersite Cooperation-Enhanced Water Splitting in Quadruple Perovskite Oxide CaCu3Ir4O12. *Chemistry of Materials* **2021**, *33*, 9295-9305, doi:10.1021/acs.chemmater.1c03015.
5. Li, X.; Wang, H.; Cui, Z.; Li, Y.; Xin, S.; Zhou, J.; Long, Y.; Jin, C.; Goodenough, J.B. Exceptional oxygen evolution reactivities on CaCoO3 and SrCoO3. *Sci Adv* **2019**, *5*, eaav6262, doi:10.1126/sciadv.aav6262.
6. Yan, J.; Xia, M.; Zhu, C.; Chen, D.; Du, F. Perovskite With Tunable Active-Sites Oxidation State by High-Valence W for Enhanced Oxygen Evolution Reaction. *Front Chem* **2021**, *9*, 809111, doi:10.3389/fchem.2021.809111.
7. Xiong, J.; Zhong, H.; Li, J.; Zhang, X.; Shi, J.; Cai, W.; Qu, K.; Zhu, C.; Yang, Z.; Beckman, S.P.; et al. Engineering highly active oxygen sites in perovskite oxides for stable and efficient oxygen evolution. *Applied Catalysis B: Environmental* **2019**, *256*, doi:10.1016/j.apcatb.2019.117817.
8. Oh, N.K.; Seo, J.; Lee, S.; Kim, H.J.; Kim, U.; Lee, J.; Han, Y.K.; Park, H. Highly efficient and robust noble-metal free bifunctional water electrolysis catalyst achieved via complementary charge transfer. *Nat Commun* **2021**, *12*, 4606, doi:10.1038/s41467-021-24829-8.
9. Long, J.; Zhang, J.; Xu, X.; Wang, F. Crystalline NiFe layered double hydroxide with large pore volume as oxygen evolution electrocatalysts. *Materials Chemistry and Physics* **2020**, *254*, doi:10.1016/j.matchemphys.2020.123496.
10. Majee, R.; Islam, Q.A.; Bhattacharyya, S. Surface Charge Modulation of Perovskite Oxides at the Crystalline Junction with Layered Double Hydroxide for a Durable Rechargeable Zinc-Air Battery. *ACS Appl Mater Interfaces* **2019**, *11*, 35853-35862, doi:10.1021/acsami.9b09299.
11. Wu, X.; Miao, H.; Hu, R.; Chen, B.; Yin, M.; Zhang, H.; Xia, L.; Zhang, C.; Yuan, J. A-site deficient perovskite nanofibers boost oxygen evolution reaction for zinc-air batteries. *Applied Surface Science* **2021**, *536*, doi:10.1016/j.apsusc.2020.147806.
12. Mondal, S.; Majee, R.; Arif Islam, Q.; Bhattacharyya, S. 2D Heterojunction Between Double Perovskite Oxide Nanosheet and Layered Double Hydroxide to Promote Rechargeable Zinc-Air Battery Performance. *ChemElectroChem* **2020**, *7*, 5005-5012, doi:10.1002/celc.202001412.
13. Göl, E.Y.; Aytekin, A.; Özkahraman, E.E.; Karabudak, E. Investigation of oxygen

evolution reaction performance of silver doped Ba0.5Sr0.5Co0.8Fe0.2O3-δ perovskite structure. *Journal of Applied Electrochemistry* **2020**, *50*, 1037-1043, doi:10.1007/s10800-020-01457-6.

14. Zhu, Y.; Chen, G.; Zhong, Y.; Chen, Y.; Ma, N.; Zhou, W.; Shao, Z. A surface-modified antiperovskite as an electrocatalyst for water oxidation. *Nat Commun* **2018**, *9*, 2326, doi:10.1038/s41467-018-04682-y.
15. Tang, D.; Liu, J.; Wu, X.; Liu, R.; Han, X.; Han, Y.; Huang, H.; Liu, Y.; Kang, Z. Carbon quantum dot/NiFe layered double-hydroxide composite as a highly efficient electrocatalyst for water oxidation. *ACS Appl Mater Interfaces* **2014**, *6*, 7918-7925, doi:10.1021/am501256x.
16. Li, G.; Hou, S.; Gui, L.; Feng, F.; Zhang, D.; He, B.; Zhao, L. Carbon quantum dots decorated Ba0.5Sr0.5Co0.8Fe0.2O3- perovskite nanofibers for boosting oxygen evolution reaction. *Applied Catalysis B: Environmental* **2019**, *257*, doi:10.1016/j.apcatb.2019.117919.
17. Hua, B.; Li, M.; Zhang, Y.-Q.; Sun, Y.-F.; Luo, J.-L. All-In-One Perovskite Catalyst: Smart Controls of Architecture and Composition toward Enhanced Oxygen/Hydrogen Evolution Reactions. *Advanced Energy Materials* **2017**, *7*, doi:10.1002/aenm.201700666.
18. Chen, G.; Zhu, Y.; Chen, H.M.; Hu, Z.; Hung, S.F.; Ma, N.; Dai, J.; Lin, H.J.; Chen, C.T.; Zhou, W.; et al. An Amorphous Nickel-Iron-Based Electrocatalyst with Unusual Local Structures for Ultrafast Oxygen Evolution Reaction. *Adv Mater* **2019**, *31*, e1900883, doi:10.1002/adma.201900883.